Effects of sintering temperature on structure of hydroxyapatite studied with Rietveld method

LINGHONG GUO*, MEI HUANG, XINGDONG ZHANG
Engineering Research Center for Biomaterials, Sichuan University, Chengdu, 610064, China
Email: guolinghong@sohu.com

It is obvious that the sintering temperature of hydroxyapatite (HA) ceramics significantly affects their biological responses *in vitro* or *in vivo*. The HA ceramics sintered at different temperatures exhibite a wide variation of biological response, but the correlation of this variation with the parameters of HA crystalline structure is not fully investigated. In present study, the crystalline structure of HA powders sintered at different temperatures at 600, 800, 1000, 1200 °C, was characterized using X-ray diffraction (XRD), and then refined with Rietveld method. A series of structure parameters, such as, cell lattice parameters (*a* and *c*) and bond length, distances of special atoms on surface to nearest atom, a numerical index of distortion for PO_4 tetrahedron, as well as internal energy and density of HA cell, were calculated to characterize the crystalline structure of HA at atom level. The broadening effect of XRD reflections was also separated to calculate the micro-strain/crystalline size, respectively. These parameters of HA crystalline structure and cell demonstrated that with rising of the sintered temperature, the internal energy and micro-strain of HA cell decreased, but the crystalline size increased. The regularity of PO_4 tetrahedron and distance between Ca_1 and O_3 in HA cell showed the same tendency as the internal energy and micro-strain with sintering temperature. All of these parameters indicated that HA became more stable with the rising of sintering temperature.

Introduction

Owing to similar with the minerals of bones and teeth in chemical composition and crystalline structure, hydroxyapatite (HA) ceramics have been widely used as bone substitutes. It was suggested that HA ceramics exhibited significantly different bioresponses *in vitro* and *in vivo* [1–3]. Ong *et al*. [1] reported that *in vitro* more differentiated osteoblasts were observed and higher alkaline phospharase-specific activity was detected on the sintered HA surface compared to the as-received HA and calcined HA surface. Best *et al*. [2] reported that osteoblast response on two kinds of HA, supplied by different manufacturers, showed significant difference. The differences in the adhesive response of epithelial cells to different crystallographic structure of HA were reported although these structures were chemically identical [3]. Above results indicate that the crystalline structure of HA may be the critical and intrinsic factor to determine its bioactivity.

Up to now, the terms of crystallinity and crystalline size have been widely used to explain the bioactivity of HA. The crystallinity is an overall index which is not directly correlated with HA crystalline structure, and its definition has also no definite meaning in crystalline structure, therefore it is not the parameter of HA crystalline structure. The crystalline size calculated with Scherrer equation is often measured by data of the full-width-at-half-maximum (FWHM) of a certain peak from X-ray diffraction (XRD) pattern of HA, such as, [0 0 2] or [2 1 1] [4]. Almost all data of crystalline size from the previous references did not consider the contribution of micro-strain to the broadening effects of reflections in XRD pattern. At same time the crystalline size calculated with Scherrer equation uses only one special reflection, not all reflections in the XRD pattern, so that the crystalline size calculated from Scherrer equation is smaller than its actual value.

It can be concluded that the HA bioactivity closely correlates with its crystalline structure, and crystallinity and crystalline size are not able to reflect the fine difference in crystalline structure of HA resulted from sintering. In order to further elucidate and understand the HA biological response *in vivo*, it may be essential to characterize these fine differences of HA structure at more advanced level.

Structure determination or characterization is the first and vital step in most materials research. Rietveld method, a method for analyzing variation and distortion of crystalline structure, is a useful tool in the field of inorganic materials and ceramics [5, 6]. It was also used in biomaterial science for quantitative phase analysis and structure refinement [7–11]. Cerius^2 (MSI, USA), a soft

*Author to whom all correspondence should be addressed.

package, provides a prefect tool to analyze crystalline structure using advanced computational methods, and to simulate, interpret, and apply data from analytical instruments, such as XRD, FTIR, TEM, etc. On the other hand, Cerius[2] also supplies a platform to build, view, and geometrically measure three-dimensional (3D) models of crystalline structure.

The objective of this study is to investigate the effects of sintering temperature on HA crystalline structure, and to introduce new quantitative parameters to discern the fine difference of HA structure resulted from sintering temperature. In this study, HA was synthesized with $Ca(NO_3)_2$ and $(NH_4)_2HPO_4$ by wet-chemical method, the as-received powder was sintered at different temperatures, 600, 800, 1000, 1200 °C. The XRD experiments were performed for sintered HA powders, and the XRD data were processed using the Rietveld method to refine the crystalline structure of HA. Rietveld refinement of structure supplied the detail information about HA crystalline structure, such as lattice parameters, crystalline size and micro-strain, bond length and angle, as well as a number index of distortion of the PO_4 tetrahedron. Based on the principle of molecular dynamics, the internal energy and density of HA cell were also calculated with Minimizer software of Cerius[2].

Materials and methods

Synthesis method of precursor powders

The precursor powders of HA were synthesized by mixing $Ca(NO_3)_2$ solution with $(NH_4)_2HPO_4$ with chemical methods at pH = 9–ll.

$$10Ca(NO_3)_2 + 6(NH_4)_2HPO_4 + 2NH_4OH = Ca_{10}(PO_4)_6(OH)_2 + 20(NH_4)NO_3 \quad (1)$$

At temperature of 60 °C, the pH of 0.5 M $(NH_4)_2HPO_4$ were adjusted to 11 with 20% NH_4OH solution, and then 0.5 M $(NH_4)_2HPO_4$ were dropped into the $Ca(NO_3)_2$ solution. During the synthesis process, the pH was monitored with a digital pH-meter and maintained at a pH range of 10–11. After precipitation, the reacting mixture was continuously stirred for 1 h and aged for 48 h. The slurry was filtered and washed four times with distilled water. The cake was dried at 80 °C, and then the precursor powders of HA were sintered in the oven in the atmosphere. The programed sintering was used to carefully control the sintering process. That is, the precursor powders of HA were sintered at a heating rate of 5 °C/min and dwelled at 600 °C (HA-6), 800 °C (HA-8), 1000 °C (HA-10), and 1200 °C (HA-12) for 2 h, respectively.

X-ray diffraction

Powders of sintered HA powders were ground and placed in the glass holder. XRD experiments were performed on using a Riguku diffractometer (D/Max 1400, CuKα 1 = 0.15405 nm, Kα2 = 0.15444 nm, 60 kV, 150 mA). Using flat plate geometry, diffraction pattern over 10–70° in 2-theta were collected with step scanning (step size = 0.02, set time = 5 s). Data were collected using a scintillation counter and a graph-diffracted beam monochromator. The peak widths were calibrated using standard curve produced from CaF_2. The characteristics of HA as determined by XRD peak broadening were used to obtain information about the crystalline size/micro-strain of the HA crystals. Because broadening effects of crystalline size and micro-strain is superimposed, the contributions of crystalline size/micro-strain to peak broadening are able to be separated with the following equation [12]

$$\beta \cos \theta/\lambda = 1/D + \varepsilon \sin \theta/\lambda \quad (2)$$

where β is the corrected the FWTH (Rad); D is the mean crystalline size and ε is the micro-strain in crystalline structure.

Structure refinement

Rietveld analysis was performed with DWBS in Cerius[2] (Version 4.2) on SGI workstation (MSI, USA). Supplied by MSI company, the starting model of 3D HA with space group P63/m with $a = 0.9421$ nm and $b = 0.6884$ nm was constructed base on the data of HA single-crystal. Fig. 1 is the starting 3D model of HA for Rietveld refinement.

In DWBS software the program uses the Newton–Raphson algorithm to minimize the intensity difference [13]:

$$S_y = \sum_i W_i (Y_i - Y_{ci})^2 \quad (3)$$

where $W_i = 1/Y_i$, and Y_i = observed intensity at the ith step, Y_{ci} = calculated intensity at the ith step

$$Y_{ci} = S \sum_j \left| N_j f_j \exp[2\pi i(hx_j + ky_j + lz_j) \exp[-B_j(\sin^2 \theta/\lambda)]^2 \Phi(2\theta_i - 2\theta_k) L_k P_k] \right| + Y_{bi} \quad (4)$$

S is a scale factor; (x_j, y_j, z_j) is the fraction coordinates of the jth atom; h, k, and l are miller indices; N_j is the site occupancy of jth atom; f_j is the scattering factors of jth atom; B_j is the isotropic temperature factors of jth atom; Φ is a reflection profile function; L_k contains the Lorentz, polarization and multiplicity factors; P_k is preferred orientation function; Y_{bi} is background intensity at ith step; θ is the diffraction angle.

The scale factors and six background factors were first refined, and then the lattice parameters were refined. For

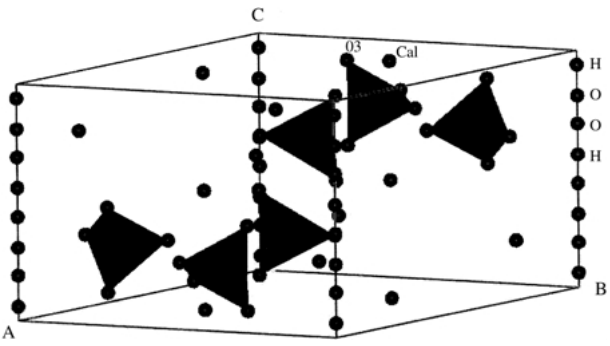

Figure 1 3-D structure of hydroxyapatite (P63/*m*, $a = 0.9421$ and $c = 0.6884$ nm) (sphere represents the atom Ca, O, H, and PO_4 tetrahedron represented the PO_4, where P atom in center of tetrahedron and O at the point of tetrahedron, OH group on the *Z*-axis).

further refinement, five parameters of peak shape were modeled based on pseudo-Voigt function. Before the refinement of the atom parameters, the orientation and isotropic temperature, zero-point, transparency, as well as asymmetry, were refined. At last the atom parameters, that is, atom coordinates, occupancy, were refined. To characterize the overall distortion of structure, the number index of distortion D_{ind}, representing the deviation of the PO_4 tetrahedron from an optimal configuration, was defined [10]:

$$D_{ind} = \sum(\theta_i - 109.17)^2/6 \quad (5)$$

where θ_i is the angle of O–P–O in the PO_4 tetrahedron; 109.17 is the degree of O–P–O in standard PO_4 tetrahedron; 6 is number of angles in PO_4 tetrahedron.

Internal energy calculation

After refinement of HA structures, the refined model was the optimum model based on XRD experimental data. The calculation of internal energy and density were performed with Minimizer, a packed molecular dynamics software in Cerius^2, under the condition of universal force field (2.1). The calculated internal energy included the contribution of chemical bonds, Van der Waales and H bonds.

Results

HA has a hexagonal space group P63/m with $a = 0.9421$ and $c = 0.6884$ nm, and ideal chemical formula is $Ca_{10}(PO_4)_6(OH)_2$. The O–H groups are ordered on the *Z*-axis, and easily replaced by other ions or ion groups, such as F^- and CO_3^{2-} ions. The Ca1 is on the surface of [0 0 1] plane and is also able to be replaced by other cation ions, such Mg^{2+} and Sr^{2+}. Fig. 1 is 3D model of HA cell based on the data. There are 6 PO_4 tetrahedrons in the cells. Two types of Ca atoms in HA cell. Ca_1 is located on the [0 0 1], and the Ca_2 are located in the cells. The fraction coordinate (*x*, *y*, *z*) of Ca_1 and Ca_2 are (0.6666; 0.3333; 0.0018) and (0.2448, 0.9879, 0.2500), respectively.

Fig. 2 was the multi-plotting of XRD patterns for HA powders sintered at different temperatures. The FWHM of the peaks decreased but intensity of each reflection

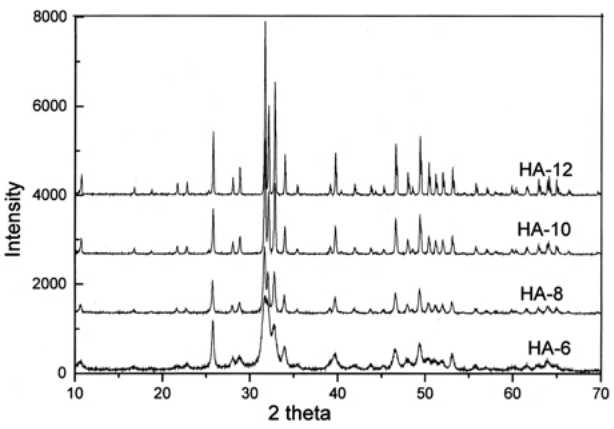

Figure 2 XRD pattern of HA samples sintered at different temperatures (HA-6, HA-8, HA-10, HA-12 were HA samples sintered at 600, 800, 1000 and 1200 °C).

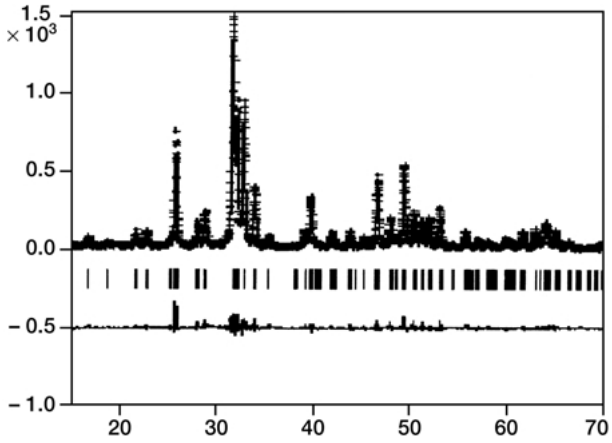

Figure 3 Rietveld refinement of HA-10.

increased with rising of sintering temperature. The XRD pattern of HA-6 exhibited a broadening at all 2θ, and a significant overlapping of peaks at 2θ range of 31.7–33°, which indicated that crystalline structure of HA sintered at 600 °C was imperfect. At 800 °C, all specific peaks of HA appeared on the XRD pattern, which showed that relatively perfect structure of apatite was established during sintering process from 600 to 800 °C. XRD qualitative analysis revealed that the sintered powders were pure HA. There were no other phases of calcium phosphates, such as β-tricalcium phosphate, calcium oxide, in all samples sintered at the temperature range of 800–1200 °C. Comparing with the *d*-values of HA, the slight peak shifts of HA sintered at different temperatures indicated that HA crystals had somewhat fine difference in crystalline structure. By means of XRD traditional analysis method, such as, qualitative analysis, calculation of crystallinity and crystal size, etc. there was no obvious difference among HA samples sintered at 800–1200 °C.

Fig. 3 showed the profile fitting of Rietveld refinement, with the observed data points overlaid with the calculated pattern, which was drawn as a solid line. The bottom horizontal line showed the difference of observed intensity and calculated intensity based on refined HA model by Rietveld refinement. This graph depicted the extent of disagreement between the refined structure model and raw XRD data of tested powders. The fitting indexes of Rietveld refinement R–P, was between 8.9 and 12 for all HA samples.

Table I listed Rietveld refinement results for dimension, density, crystalline size and micro-strain of crystalline cell and R–P etc. from 600 to 800 °C. From the Table I, it was obvious that the axis of unit cell (a) increased significantly from 0.936960 to 0.939630 nm. The reason of this significant variation could be attributed to the transformation of semi-amorphous apatite (imperfect) to crystalline hydroxyapatite about 750 °C [14]. From 800 to 1200 °C, there was no significant variation of an axis and c axis for HA unit cell.

Fig. 4 was representative graph of FWHM vs the diffraction angle in order to separate the broadening effects of main peaks of crystalline size form micro-strain because the broadening effect of XRD peaks was resulted from both crystalline size and micro-strain [12]. The data of FWHMs of reflections corresponding to the diffraction angles were plotted to calculate the crystalline

TABLE I Results of Riteveld refinement and the related calculations

Sample	R–P (%)	Lattice parameter (nm)		Density (g/cm^3)	Isotropic temperature factors	Internal energy (kcal/mol)	Crystalline size (nm)	Lattice strain (%)
		a	*c*					
HA-6	12.38	9.36960	6.84690	3.3133	1.68530	3766.34	35.84	0.22950
HA-8	9.84	9.39590	6.86630	3.2831	2.05540	3694.80	42.70	0.03525
HA-10	9.29	9.39630	6.86620	3.2830	4.22910	3458.34	48.30	−0.06625
HA-12	12.60	9.42340	6.88290	3.2590	4.50200	3445.81	57.14	−0.06250

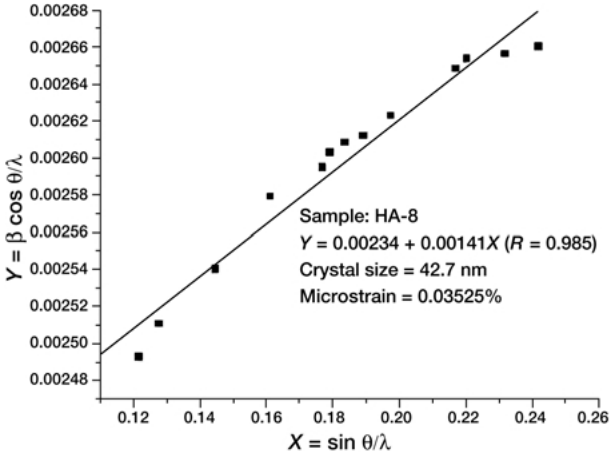

Figure 4 Separation of the micro-strain and crystalline size for HA-8.

size and micro-strain of HA crystals from the slope and intercept of the curve, respectively. With sintering temperature increasing, the crystalline size constantly increased, but the micro-strain decreased. The increase of the crystalline size and decrease of the micro-strain of HA directly resulted in the increased stability, respectively.

Table II listed other results of Rietveld refinement related with HA crystalline structure at atom level, such as the bond length and angles of PO_4 tetrahedron. The Ca_1 was the activist part in HA structure because they were on [0 0 1] plane of crystalline structure and easy to replace or exchange with other ions or ion groups. The distance between Ca_1 and nearest O_3 in the HA cell may be a quantitative index to characterize the inter-action of Ca_1 and its nearest atom O_3, which closely related to the activity HA. As rising of sintering tempera-ture, the distance between Ca_1 and O_3 steadily decreased.

At 600 and 800 °C the tetrahedron of PO_4 was relatively irregular, that is, the differences of P–O bond angles were relatively greater because P–O lengths were slightly different. Lopes *et al*. [7] also found that bond length of Ca_2 and Ca_2 decrease with firing temperature at the range of 1200–1350 °C.

With the elevation of sintering temperature, the tetrahedron of PO_4 became more regular. D_{ind}, the number index of distortion of the PO_4 tetrahedron, showed the tendency to lower as the increase of sintering temperature. The variation in distortion index (%) of the prepared materials with respect to sintering temperature was also shown in Table II. In general, the distortion index of HA sintered at 1200 °C was found to be significantly lower than the distortion index of the materials sintered at 600 °C. Jha *et al*. [10] used the D_{ind} to characterize the distortion of HA and fluoride-substituted apatite (FHA) synthesized in solution at different temperatures, such as 0 °C, 90 °C. The D_{ind} value of HA for 0 and 90 °C was about 18 and 8, respectively [10]. The D_{ind} of this study agreed with Jha's results. The D_{ind} of sintered HA was smaller than these of synthesized HA at lower temperature. Comparing with D_{ind} of HA samples synthesized and sintered, it was obvious that the effects of temperature greatly affected the distortion of PO_4 tetrahedron. But Comodi *et al*. [15] found that the PO_4 tetrahedron did not show clear trend toward regularization under pressure, even at high pressure (7 GPa).

In molecular dynamics theory, the thermal motion of the constituent atoms is simulated by numerically integrating Newton's second law of motion. Molecular dynamics approximates energy by summing a series of empirical terms representing the chemical, and electro-static interaction in molecular or crystal system. Minimizer of Cerius^2 is software to minimize the energy for certain molecular or crystals based on the molecular dynamics. The internal energy calculated for the refined HA cell decreased with rising of sintering temperature. The internal energy may be used as an overall index for stability, that is, higher internal energy means lower stability. The internal energy revealed the relationship of structure and behavior, and was also able to provide insight into key molecular and predicted critical properties. Lench [16] and West *et al*. [17] have tried to use molecular model to calculate the interaction of bioglass and ploy-L-lysine, one of basic units composed of proteins, and their computation were conformed to their experimental results. The energy of bioglass and ploy-L-lysine system was used to determine whether the reaction took place in the system [17].

TABLE II Bond lengths and distortion index

Spec.	P–O_1 (nm)	P–O_2 (nm)	P–O_3^* (nm)	Ca_1–O_3 (nm)	Distortion index (%)
HA-6	0.1501	0.1507	0.1553	0.2819	5.0533
HA-8	0.1518	0.1502	0.1532	0.2817	3.8751
HA-10	0.1536	0.1529	0.1536	0.2806	2.3186
HA-12	0.1536	0.1507	0.1504	0.2800	0.4781

*Repeated by symmetry.

The calculated density listed in Table I showed that the unit cell of HA contracted with elevated sintering temperature. The calculated density, a widely used popular term, might reflect the geometrical compacting property of atoms in the cell and the regularity of structure. A slight higher density meant that there was more strong interaction among atoms in the cells. For same materials, such as HA, decrease of density indicated its stability increased, so that the HA stability would improve with the increase of sintering temperature.

Discussion

As bone replacement materials and potential scaffold matrixes for bone tissue engineering, HA and calcium phosphates related materials have attracted extensive research. Although used as bioactive bone substitute, poor mechanical properties of HA limited its application. To produce ceramics and improve their mechanical properties, the sintering process is an essential step. The higher sintering temperature would improve mechanical performance of HA ceramics, but deteriorate its bioactivity. To investigate the effects of sintering temperature on HA crystal structure may be the best way to solve the contradictory of mechanical property and bioactivity of Ha ceramics.

Depending on HA properties, the different rates of cellular response have been observed *in vitro* or *in vivo* [1–3]. These differences have often been contributed to the variation of surface properties and crystallinity qualitatively. Although *in vivo* bioresponse of HA is complex and controlled by many factors of hosts and HA implants, the quantitative and more detail characterization for HA may be the first and crucial step to explain bioresponse of HA implant. On the other hand, the various apatites, such as calcium-deficient apatite, carbonated apatite, fluorapatite etc. are often produced depending on the synthesizing parameters. In chemical methods of HA preparation, various amount of water and hydrogen phosphate, as well as carbonate, are unavoidable to be retained in apatite structure of the synthesized HA powders, therefore, the different sources of HA produced a wide variation of bioresponse. The complex chemistry of HA also makes it difficult to correlate its bioresponse *in vitro* and *in vivo* to its chemical property. Because the complex of bioresponse process *in vivo* and chemistry of HA, the detail investigation of HA structure seems to be of importance to explain the bioactivity of HA *in vivo*.

Higher sintering temperature result in higher crystallinity, therefore, it is inferred that the Ca^{2+} and PO_4^{3-} is more difficult to dissolve. Although the crystallinity and crystalline size have been widely used to explain the different dissolution of HA, these explanations are not satisfied to explain some observed results of the experiment because they does not explain these phenomena at atom level based on crystal structure. It was objective for this study to find more reasonable explanation. In this study, some new parameters of structure were introduced in order to correlate HA stability with its crystal structure. The internal energy and density of cell were overall indexes of HA stability, and distortion index D_{ind} and length between atoms were parameters of structure at atom level. Comparing with crystalline size calculated by Scherrer equation, the values from Rietveld refinement and Equation 2 was more reasonable. All these data were agreed with the tendency of bioactivity. Recently there has been a tendency to use molecular modeling to simulate the bioresponse and biomimetic process by calculating the interaction of proteins and materials [16–18].

It is widely accepted that the early interaction of proteins and HA determined its bioresponse *in vivo*. Using molecular modeling, Laila Huq *et al*. [18] reported the preferences of multiphosphorylated motif Glu–Glu–Ser(P)–Ser(P)–Ser(P) of proteins and peptides for [1 0 0] and [0 1 0] surfaces of the HA crystal and preferences for particular orientations on a given surface. These preferences are principally governed by electrostatic interactions between the crystal lattice and the peptide with the most stable conformers adopting structures where alternate residues exhibit backbone angles characteristic of a β-strand and values of an α-helix or a distorted α-helix, allowing maximal interaction between the acidic side groups and surface calcium atoms. The spatial positions and distance between atoms at specific surface in HA cell and the distortion of PO_4 tetrahedron probably affects the interaction of proteins and HA, so that this preliminary study may supply some information about HA crystal structure at atom level to help explain interaction of proteins and HA.

In summary, sintering process improved the stability of HA which may resulted in the decrease of bioactivity. The sintering process from 600 to 1200 °C might be divided into three stages. From 600 to 800 °C, significant change of a, as well as Dind and internal energy E, indicated that the obvious change in structure was occurred, that is the semi-crystal transform into perfect crystal, similar with crystallization process. From 800 to 1000 °C, the sintering mainly improved the perfecting of cell. From 1000 to 1200 °C, there were no significant change for all indexes, this process may be classified as the densing process in order to fabricated the HA ceramics with suitable mechanical properties.

Conclusion

The results of Rietveld refinement verified that the fine microstructure of HA sintered at different temperatures was somewhat different. The results of internal energy calculation and the number index of distortion of PO_4 tetrahedron, as well as crystalline size, micro-strain, etc., indicated that stability of HA increased with the rising of sintering temperature. From the view of crystalline structure Rietveld refinement supplied the quantitative results about crystal structure of HA at atom level. These results may be used to explain the *in vivo* different responses of HA sintered at different temperature.

References

1. J. L. ONG, C. A. HOPPE, H. L. CARDENAS, R. CAVIN D. L. SOGAL and G. N. RAIKAR, *J. Biomed. Mater. Res.* **39** (1998) 176.

2. S. BEST, B. SIM, M. KAYSER and S. DOWNES, *J. Mater. Sci.: Mater. Med.* **8** (1997) 97.
3. Y. HARADA, J. T. WANG, DOPPALAPUDI, A. A. WILLIS, M. JASTY, W. H. HARRIS, M. NEGASE, S. R. GOLDRING, *J. Biomed. Mater. Res.* **31** (1996) 19.
4. S. ZHANG, GONSALVES *J. Mater. Sci.: Mater. Med.* **8** (1997) 25.
5. R. L. MILLARD, R. C. PETERSON and B. K. HUNTER, *Am. Mineral.* **80** (1995) 885.
6. V. RAMASWAMY, L. B. MCCUSKER and C. H. BAERLOCHER, *Micro. and Mesop. Mater.* **31** (1999) 1.
7. M. A. LOPES, J. D. SANTOS, F. J. MONTEIRO and J. C. KNOWLES, *J. Biomed. Mater. Res.* **39** (1998) 244.
8. L. KULLER, *ibid.* **29** (1995) 1403.
9. H. MORGAN, R. M. WILSON, J. C. ELLIOTT, S. E. P. DOWKER and P. ANDERSON, *Biomaterials* **21** (2000) 617.
10. L. J. JHA, S. M. BEST, J. C. KNOWLES, I. REHMAN, J. D. SANTOS and W. BONFIELD, *J. Mater. Sci.: Mater. Med.* **8** (1997) 185.
11. I. ABRAHAMS and J. C. KNOWLES, *J. Mater. Chem.* **4** (1994) 185.
12. H. P. KLUG, L. E. ALEXANDER, in ''X-ray Diffraction Procedures for Polycrystalline and Amorphous Materials'' (John Wiley & Son, 1974).
13. R. A. YOUNG, A. SAKTHIVEL, T. S. MOSS, Paiva-Santos CO, User's Guide to Program DWBS-9411.
14. J. M. ZHOU, X. D. ZHANG, J. CHENG, S. ZENG and K. DE GROOT, *J. Mater. Sci.: Mater. Med.* **4** (1993) 83.
15. P. COMODI, YU LIU, P. F. ZANNAZZI, M. MONTAGNOLI, *Phys. Chem. Min.* **28** (2001) 219.
16. L. L. LENCH, Proceeding of 5th World Congress on Biomaterials, Toronto, Canada, K6, 1996.
17. J. K. WEST, R. J. LATOUR and L. L. HENCH, *J. Biomed. Mater. Res.* **37** (1997) 585.
18. N. LAILA HUQ, KEITH J. CROSS and ERIC C. REYNOLDS, *J. Mol. Model.* **6** (2000) 35.

Received 15 August 2000
and accepted 4 February 2003